

Atomic radius and charge parameter uncertainty in biomolecular solvation energy calculations

Xiu Yang^{1,*}, Huan Lei^{1,*}, Peiyuan Gao¹, Dennis G. Thomas²,
David Mobley³, and Nathan A. Baker^{1,4,5}

*These authors contributed equally.

¹Advanced Computing, Mathematics, and Data Division, Pacific Northwest National Laboratory, Richland, WA 99352, USA

²Biological Sciences Division, Pacific Northwest National Laboratory, Richland, WA 99352, USA

³Department of Pharmaceutical Sciences, University of California Irvine, Irvine, CA 92697, USA

⁴Division of Applied Mathematics, Brown University, Providence, RI 02912, USA

⁵Contact information: nathan.baker@pnnl.gov, +1-509-375-3997

December 25, 2017

Abstract

Atomic radii and charges are two major parameters used in implicit solvent electrostatics and energy calculations. The optimization problem for charges and radii is under-determined, leading to uncertainty in the values of these parameters and in the results of solvation energy calculations using these parameters. This paper presents a new method for quantifying this uncertainty in implicit solvation calculations of small molecules using surrogate models based on generalized polynomial chaos (gPC) expansions. There are relatively few atom types used to specify radii parameters in implicit solvation calculations; therefore, surrogate models for these low-dimensional spaces could be constructed using least-squares fitting. However, there are many more types of atomic charges; therefore, construction of surrogate models for the charge parameter space requires compressed sensing combined with an iterative rotation method to enhance problem sparsity. We demonstrate the application of the method by presenting results for the uncertainties in small molecule solvation energies based on these approaches. The method presented in this paper is a promising approach for efficiently quantifying uncertainty in a wide range of force field parameterization problems, including those beyond continuum solvation calculations. The intent of this study is to provide a

way for developers of implicit solvent model parameter sets to understand the sensitivity of their target properties (solvation energy) on underlying choices for solute radius and charge parameters.

1 Introduction

Implicit solvent models and their applications have been the subject of numerous previous reviews [1–3]. Such solvation models require the coordinates of the solute atoms as well as atomic charge distributions and a representation of the solute-solvent interface. Charges and interfaces are generally modeled through parameterized empirical representations; however, these parameterizations are often under-determined, leading to uncertainty in the resulting parameter sets [4–6]. The Poisson equation is a popular model for implicit solvent electrostatics and serves as a good example for exploring the influence of this uncertainty on properties such as molecular solvation energy [1–3, 7]. In this paper, we use the term “solvation energy” to refer to the energy returned from the Poisson equation and to emphasize that we are not sampling over solute conformational states for a true *free* energy. This is a partial differential equation for the electrostatic potential $\varphi : \Omega \mapsto \mathbb{R}$

$$\begin{aligned} -\nabla \cdot \epsilon(\mathbf{x}) \nabla \varphi(\mathbf{x}) &= \rho(\mathbf{x}) \text{ for } \mathbf{x} \in \Omega & (1) \\ \varphi(\mathbf{s}) &= \varphi_D(\mathbf{s}) \text{ for } \mathbf{s} \in \partial\Omega, & (2) \end{aligned}$$

where $\Omega \subset \mathbb{R}^3$ is the problem domain, $\partial\Omega$ is the domain boundary, $\epsilon : \Omega \mapsto [1, \infty)$ is a dielectric coefficient, $\rho : \Omega \mapsto \mathbb{R}$ is the charge distribution, and φ_D is a reference potential function (e.g., Coulomb’s law) used for the Dirichlet boundary condition. The dielectric coefficient ϵ is usually defined implicitly [8–11] with respect to the solute atomic radii $\{\sigma_i\}$ and solvent properties such that the coefficient reaches two limiting constant values: ϵ_u inside the solute and ϵ_v away from the solute in bulk solvent. The solvation energy is calculated by

$$\Delta G = \int_{\Omega} \rho(\mathbf{x}) (\varphi(\mathbf{x}) - \varphi_0(\mathbf{x})) d\mathbf{x}, \quad (3)$$

where φ is the Poisson equation solution for the system with a bulk value of ϵ corresponding to the solvent of interest and φ_0 is the solution for the system with a bulk value of ϵ corresponding to a vacuum. For atomic monopoles, the solute charge distribution has the (numerically unfortunate) form $\rho(\mathbf{x}) = \sum_i^{N_A} q_i \delta(\mathbf{x} - \mathbf{x}_i)$ for N_A solute atoms with positions $\{\mathbf{x}_i\}$ and charges q_i . The δ terms are formally defined as Dirac delta functionals but usually approximated by functions with finite support (e.g., when projected onto a grid or finite element basis). The delta functional approximation leads to a simplified form for the solvation energy in Eq. 3,

$$\Delta G = \sum_i^{N_A} q_i (\varphi(\mathbf{x}_i) - \varphi_0(\mathbf{x}_i)). \quad (4)$$

Charges and interfaces in implicit solvent representations are generally modeled through parameterized empirical representations; however, these parameterizations are often under-determined leading to uncertainty in the resulting parameter sets [4–6]. For example, atomic charge models are designed to approximate the “true” vacuum electrostatic potential due to quantum mechanical electron and nuclei charge distributions. While quantum mechanical charge distributions can be incorporated directly in implicit solvent models [12, 13], atomic point charge distributions are generally used [2]. These point charges can include inducible and fixed multipoles [14, 15] but monopoles are the most common form. For the purposes of assigning charges, atoms are grouped into sets based on molecular connectivity and environment [16]. The charge values for atoms in these sets are usually determined by numerical fitting to quantum mechanical vacuum electrostatic potentials. Such charge optimization is ill-posed and fitting requires careful choice of the objective function and regularization constraints [17–20]. While sophisticated fitting procedures have been developed, significant information reduction occurs in the transformation of the continuous quantum mechanical electron density into a discrete set of atomic point charges.

Solute-solvent interface models are much more empirical than the charge distribution models; the definition of a solvent “interface” is imprecise at length scales comparable to the size of water molecules. Therefore, such models are generally developed to represent a reasonable description of the solute geometry while also optimizing agreement with experimental quantities such as solvation energy. A large number of solute-solvent interface models exist, including van der Waals [11], solvent-accessible [21], solvent-excluded (or Connolly) [22], Gaussian-based [23], spline-based [24], and differential geometry surfaces [10, 25–29]. All of these interface models represent atoms as spheres and require information about the radii of these spheres. These radii are generally assigned to sets of atoms based on their “type” as determined by the local molecular connectivity. Unlike atomic charges, there are relatively few sets of atom types used to assign radii [16, 30]. These radii parameters are determined by optimization of properties such as solvation energy against experimental data [16, 30]. Additionally, many of these models also require information about solvent characteristics, generally in the form of a solvent radius, characteristic solvent length scales, or bulk solvent pressure/surface tension properties.

The intent of this study is to provide a way for developers of implicit solvent model parameter sets to understand the sensitivity of their target properties (solvation energy) on underlying choices for solute radius and charge parameters. In the present work, we present a new method to quantify the uncertainty in solvation energy calculated by the Poisson equation and induced by the uncertainty of the input radii and charge parameters. In particular, we construct two surrogate (or statistical regression) models of the solvation energy in terms of the radii and the atomic charges, respectively. These surrogate models enable us to estimate the solvation energy with different input parameters quickly and to evaluate the statistical information of the target properties (e.g., probability density function) efficiently. We model the input parameters as independent

(i.i.d.) Gaussian random variables with different means and standard deviations; however, other probability distributions can also be used. To construct the surrogate of the Poisson model, we use a generalized polynomial chaos (gPC) [31, 32] expansion to represent the dependence of the solvation energy on uncertain parameters such as the atomic charge and radii. The efficacy of the gPC method for elliptic problems such as the Poisson equation has been extensively studied with robust results for its efficiency and accuracy [33, 34]. This approach is straightforward to apply to the relatively low-dimensional parameter sets. However, the main challenge of applying this method to implicit solvent calculation parameter uncertainty is the high-dimensionality of parameter sets (especially the atomic charges): the surrogate models require more basis functions and, therefore, more expansion coefficients need to be identified. To address this challenge, we adopt a compressive sensing method combined with the rotation-based sparsity-enhancing method first proposed by Lei et al. [35] and extended by Yang et al. [36], which enable us to construct the surrogate with relatively few sample outputs of the numerical Poisson solver.

2 Methods

We demonstrated the framework using a test set of 17 compounds from the SAMPL computational challenge for solvation energy prediction [16] (see Table 1). This set was chosen to demonstrate the uncertainty quantification framework on several different molecules; however, it was not chosen to calculate statistics over this small set. We use this subset of the SAMPL data to demonstrate the use of our method to quantify uncertainty in solvation energy due to implicit solvent parameter uncertainty.

2.1 Uncertain parameters

Many parameterization approaches for atomic charge use ESP (electrostatic potential) [38] or related methods (e.g., RESP [19]). These methods optimize atomic charges by least-squares fitting of the charges’ Coulombic potential to the electrostatic potential obtained from quantum mechanical calculations. This under-determined optimization is performed subject to various constraints, including the requirement that the atomic charges sum to the integer formal charge of the molecule. More specifically, the calculated ESP \hat{V}_i at the i -th grid point is the electrostatic potential given by Coulomb’s law summed over the charge q_j at the centers of the j -th atoms. Least-squares fitting is performed by minimizing $\sum_i (V_i - \hat{V}_i)^2$ with constraints, where V_i is the electrostatic potential computed by *ab initio* calculations. Least-squares fitting implies a Gaussian noise model wherein the atomic charges q_j can be modeled as Gaussian random variables as done in this study.

In the present work, we modeled the uncertainty in atomic charges by considering atomic charges obtained by 11 different approaches: AM1BCC [39], CHELP [40], CHELPG [41], CM2 [42], ESPMK [38], Gasteiger [43], PCMESP [44],

Table 1: List of 17 compounds from the SAMPL computational challenge for solvation energy prediction with solvation energy [16] and solvent accessible volume from APBS [37].

Ind.	Compound	Solvation energy (kJ/mol)	Molecular volume (\AA^3)
1	glycerol triacetate	-36.99	215.80
2	benzyl bromide	-9.96	126.98
3	benzyl chloride	-8.08	124.66
4	<i>m</i> -bis(trifluoromethyl)benzene	4.48	290.91
5	<i>N,N</i> -dimethyl- <i>p</i> -methoxybenzamide	-46.07	188.44
6	<i>N,N</i> -4-trimethylbenzamide	-40.84	179.62
7	bis-2-chloroethyl ether	-17.70	121.45
8	1,1-diacetoxyethane	-20.79	148.50
9	1,1-diethoxyethane	-13.72	132.75
10	1,4-dioxane	-21.13	87.86
11	diethyl propanedioate	-25.10	165.44
12	dimethoxymethane	-12.26	81.90
13	ethylene glycol diacetate	-26.53	148.10
14	1,2-diethoxyethane	-14.81	132.91
15	diethyl sulfide	-6.49	108.15
16	phenyl formate	-15.98	126.25
17	imidazole	-41.05	67.36

Qeq [45], RESP [19], MMFF94 [46], Mulliken [47]. The Hartree-Fock method and the 6-31G* basis set were used to optimize molecular geometries. The methods we selected here are popular for implicit solvation models and all-atom approaches. Although many of these charge methods are used in all-atom simulations, implicit solvent models have been used with several of them, including RESP and ESP(MK) [30, 48], AM1-BCC [48], Mulliken [49], CHELPG [49, 50], Gasteiger [51], Qeq [52], etc.

We have *assumed* that the variation of atomic charges across different methods can be modeled by a Gaussian random field with covariance kernel

$$\text{Cov}(\mathbf{x}_i, \mathbf{x}_j) = \eta_i \eta_j \exp\left(-\frac{\|\mathbf{x}_i - \mathbf{x}_j\|_2^p}{\theta}\right), \quad (5)$$

where η_i is the standard deviation of the i -th atomic charge, \mathbf{x}_i is the position of the i -th atom, and $0 < p < 2$. The least-squares nature of most charge fitting methods makes Gaussian variables a natural choice; however, other probability distributions can also be used. We used atomic charges from 11 different methods to estimate η_i and then used the maximum likelihood estimate (MLE) method to estimate θ and p . Since the sum of N_A charges in a molecule is constrained (to its formal molecular charge $Q \in \mathbb{Z}$), we modeled the Gaussian random field with $N_A - 1$ atoms by removing the last hydrogen in the PDB file. Additionally, we use symmetry in the molecular structure to reduce the number of independent atomic charge types before applying the MLE to identify the random field. For example, in a benzene, there is only one type of carbon and one type of hydrogen due to the symmetry of this molecule. Therefore, we considered the charges of its atoms as a Gaussian random field with only two entries instead of 12 ones (the total number of atoms in benzene).

After obtaining the covariance matrix by integrating across methods, we represented the atomic charge as

$$\mathbf{q} = \langle \mathbf{q} \rangle + \mathbf{L}_c \boldsymbol{\gamma}, \quad (6)$$

where $\mathbf{q} = (q_1, q_2, \dots, q_{N_A-1})$ are the atomic charges, $\langle \mathbf{q} \rangle$ is the mean of \mathbf{q} estimated from the 11 different charge values, $\boldsymbol{\gamma} = (\gamma_1, \gamma_2, \dots, \gamma_{N_A-1})$ are i.i.d. zero-mean unit-variance Gaussian random variables, and \mathbf{L}_c is a lower triangular matrix from the Cholesky decomposition of the covariance matrix (Eq. 5). We note that for the atoms in the test set used in the present work, the covariance matrices of these random field are almost diagonal: the off-diagonal entries are smaller than 10^{-12} . This suggests the correlation between atomic charges is effectively removed during their symmetry-based grouping. The atomic charge for the remaining atom is obtained by summation of the other random charge variables based on the constraint $q_i = Q - \sum_{j \neq i}^{N_A} q_j$.

Similarly, we used multiple force fields (ZAP-9 [16], OPLSAA [53], Bondi [54] and PARSE [30]) to model uncertainty in the radii parameters in the same manner. Although radii are non-negative, we did not explicitly impose constraints on the radii. After obtaining the covariance matrix, we represented the radii as

$$\boldsymbol{\sigma} = \langle \boldsymbol{\sigma} \rangle + \mathbf{L}_r \boldsymbol{\zeta}, \quad (7)$$

where $\boldsymbol{\sigma} = (\sigma_1, \dots, \sigma_{N_A})$, σ_i is the radius of atom (type) i , $\boldsymbol{\zeta} = (\zeta_1, \dots, \zeta_{N_A})$ are independent zero-mean unit-variance Gaussian random variable and \mathbf{L}_r is a lower triangular matrix from the Cholesky decomposition of the covariance matrix. The small number of radii sets makes the selection of a probability distribution somewhat arbitrary. We have *assumed* that the radii follow a Gaussian distribution; however, other probability distributions can also be used. We note that the standard deviations here are smaller than 10% of the mean values which implies very low probabilities for unphysical negative radii values. Therefore, by employing truncated Gaussian random variables within 4 standard deviations (capturing more than 99.99% of the probability), we guaranteed that the radii are always positive and that the distributions of the truncated Gaussian variables were almost identical to the original Gaussian variates. We note that with this setting, no model assigns zero radius to protons or other atoms.

Although we use γ and ζ to denote the random variables used for modeling the uncertainties in q_j and σ_j , in what follows, we still use $\boldsymbol{\xi} = (\xi_1, \xi_2, \dots)$ to denote general uncertain inputs when introducing the algorithm and reporting results.

2.2 Solvation energy surrogate models

We used generalized polynomial chaos (gPC) expansions as surrogate models for the solvation energy. The goal of surrogate construction is to estimate the variations in quantities of interest, such as solvation energy, much more efficiently than solving the original problem, such as solving the Poisson equation. The details for these expansions are provided in Supporting Material.

2.3 Poisson equation solver

We used the Adaptive Poisson-Boltzmann Solver (APBS) [37] to solve the Poisson equation for solvation energies. Poisson calculations were performed with the finite difference solver using 97^3 grids focused from a 25 \AA to a 13 \AA cubic domain. Charges were discretized onto the grids using linear interpolation. Boundary conditions were assigned using a sum of Coloumb potentials. The molecular interior and solvent were assigned dielectric values of 2.0 and 78.0, respectively. The solute-solvent boundary was defined using a ‘‘Connolly’’ molecular surface [55]. Energies were calculated using the standard approach for Poisson-Boltzmann calculations [56, 57].

3 Results and discussion

For each test case, we used Monte Carlo simulations to sample the parameter probability distributions and generate 10,000 samples of the input parameters $\boldsymbol{\xi}^q$ and then solved PB equation using APBS to obtain output samples of the solvation energy $E^q = E(\boldsymbol{\xi}^q)$. We used these outputs as ground-truth reference solutions to examine the performance of the surrogate models; these outputs will

be referred to as “reference” in the remainder of this paper. More precisely, given a surrogate model \tilde{E} , we use two different root-mean-squared error (RMSE) measures to examine its accuracy:

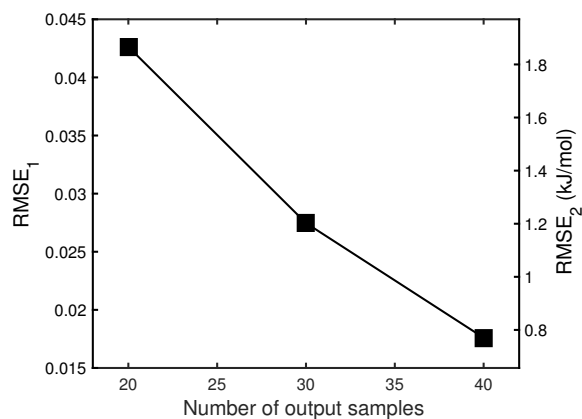
$$RMSE_1 = \sqrt{\frac{\sum_{q=1}^{10000} (\tilde{E}(\xi^q) - E^q)^2}{\sum_{q=1}^{10000} (E^q)^2}}, \quad RMSE_2 = \sqrt{\frac{\sum_{q=1}^{10000} (\tilde{E}(\xi^q) - E^q)^2}{10000}}. \quad (8)$$

We also use box-whisker plots to demonstrate the statistics. The line in the middle is the median of 16 molecules, the tops and bottoms of the boxes are 25th and 75th percentiles, and the whisker plots cover more than 99% probability.

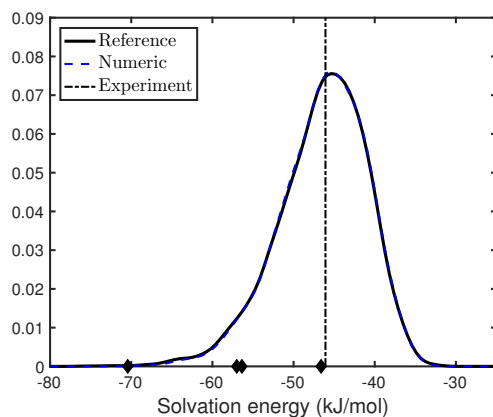
3.1 Influence of radii uncertainties on solvation energies

We investigated the effect of the uncertainties in the radii with fixed atomic charges obtained from AM1-BCC [39]. As an example, there are eight different sets of radii for *N,N*-dimethyl-*p*-methoxybenzamide across the ZAP-9, Bondi, OPLSAA, and PARSE parameter sets, as shown in the support material. We modeled the solvation as a function of eight i.i.d. Gaussian random variables. We constructed gPC surrogate models with multi-variate normalized Hermite polynomials up to third order. The surrogate model consisted of $C_{8+4}^4 = 495$ basis functions. Figure 1 (a) presents the RMSE obtained by our method with respect to different numbers of samples E^q . Figure 1 (b) compares the solvation energy probability distribution function (PDF) obtained by our method and the reference solutions. The numerical results are obtained by constructing the surrogate model with the 36 output samples first, then sampling the surrogate model 10,000 times with random samples to estimate the PDF. The reference solution is computed from the 10,000 outputs of E^q .

We performed the same analysis for all the molecules in the test set and present the results in Figure 2. For most molecules, we can build an accurate surrogate model (RMSE < 0.05) for the solvation energy with only a few samples (less than 40) of the input parameters. However, *m*-bis-trifluoromethylbenzene (TFMB) required significantly more samples. In particular, the RMSE for the TFMB solvation energy surrogate model was close to 0.15 with 40 samples and required 100 samples to reduce the RMSE to less than 5%. This variability arises from the radius of fluorine: in the ZAP force field it is 2.4 Å; however, it is only ~ 1.4 Å for the other force fields. Hence, the standard deviation of this radius is around 25% of the mean and fluorine requires more terms in the surrogate model for an accurate description and therefore more samples to parameterize those terms. The influences of the uncertainties in the input radii on the solvation energy for each molecule are demonstrated in box-whisker plots in Figure 3. The experiment results are presented for comparison. We note that some experiments results are “outliers” of the box-whisker plots, this is because that the atomic charges are computed from AM1BCC for the purpose of fixing the atomic charges and it does not guarantee that the computed solvation



(a)



(b)

Figure 1: Performance of the surrogate model for radii uncertainties for *N,N*-dimethyl-*p*-methoxybenzamide. (a): RMSE with different numbers of samples M . (b): comparison of the solvation energy PDFs estimated by the numerical surrogate method (“Numeric”) based on 40 output samples of APBS; dash line (“Experiment”) is the experimental result; diamonds are the results by using radii from ZAP-9, Bondi, OPLSAA and PARSE, respectively. The diamond closest to the experiment was obtained from ZAP-9.

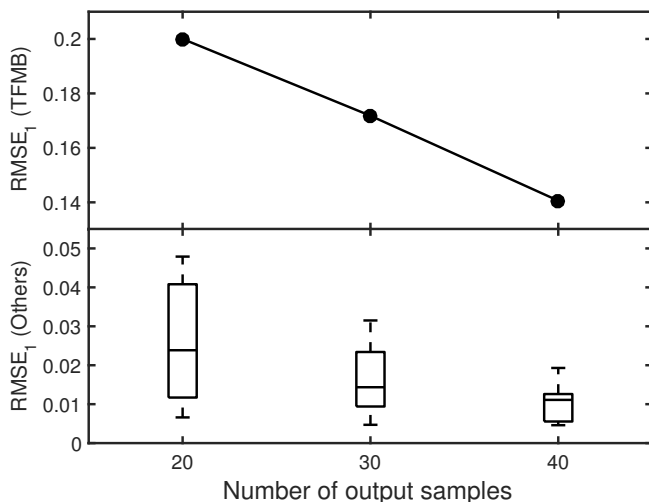


Figure 2: Performance of surrogate models with respect to number of samples. Circles are the $RMSE_1$ of *m*-bis-trifluoromethylbenzene (TFMB), box-whisker plots are the $RMSE_1$ of the remaining 16 molecules.

energy is sufficiently close to the experiment results. For example, for the *m*-bis(trifluoromethyl)benzene AM1BCC charges yield negative solvation energy while the experiment result is positive.

3.2 Influence of atomic charge uncertainties on solvation energies

We also examined the influence of charge perturbation for solvation energy calculations with fixed radii (ZAP-9). As an example, there are 14 different types of atoms in *N,N*-dimethyl-*p*-methoxybenzamide as shown in Supporting Material. We note that we model the surrogate with 13 inputs due to the constraint on the summation of the charges. The mean and standard deviation are computed from the results of 11 different charge fitting approaches. We used no more than 3000 multi-variate normalized Hermite polynomials (up to fourth order) in the gPC surrogate model for E_g for all the molecules. We use *N,N*-dimethyl-*p*-methoxybenzamide as an example. Figure 4 (a) presents the RMSE obtained by our method with respect to different numbers of samples E^q . It illustrates that 300 output samples are needed to reduce the RMSE to less than 5%. Figure 4 (b) compares the PDF obtained by our method and the reference solution. The numerical results are obtained by constructing the surrogate model with the 300 output samples first, then sampling the surrogate model 10,000 times with random samples to estimate the PDF. The reference solution is computed from the 10,000 outputs of E^q .

The influences of the uncertainties in the input atomic charges on the solva-

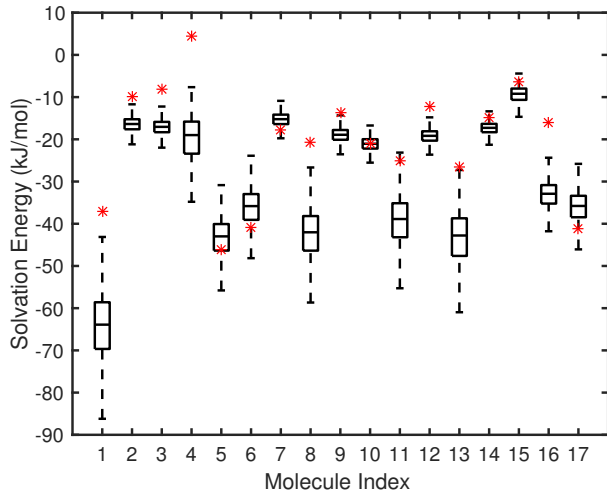


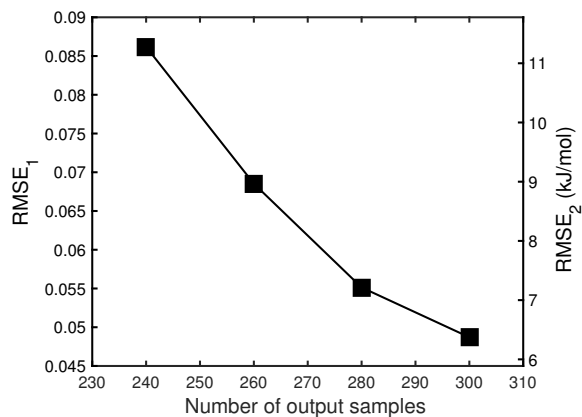
Figure 3: Influence of radii uncertainties on molecular solvation energies for the 17-molecule test set. The red stars are the experiment results.

tion energy for each molecule are demonstrated in Figure 5. For most molecules, the experiment results lie in the whisker plots and some of them are in the box. We also present the number of output samples needed to construct a surrogate with RMSE less than 5% with respect to the number of atom types in Figure 6.

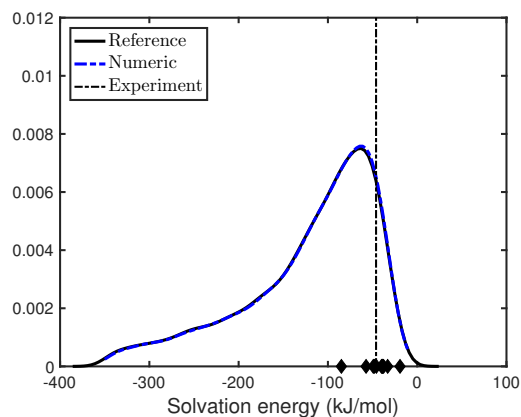
3.3 Combined influence of radius and atomic charge uncertainties

We chose the charge methods and radii based on their popularity in the implicit solvent community. Not all of the radii and charges examined in this study would be expected to give accurate answers when used together. We could have chosen a more constrained set; however, we chose this diverse set as a more challenging example to test our method to illustrate our approach across significant variation in parameter values. Comparing the PDFs in Figures 1 (b) and 4 (b), we notice that the uncertainty in the solvation energy induced by the atomic charges is stronger than that induced by the radii. A similar observation has been made previously by Chakavorty et al. [58] who also noted that conformation introduces another important source of uncertainty across force fields. We have investigated the influence of conformational uncertainty on solvation in a previous paper using similar methods [35]; however, combining parameter and conformational uncertainty is outside the scope of this manuscript.

The atomic charges vary significantly across different methods while the variation in the radii is much smaller. To understand the combined influence of charges and radii on solvation energies, we modeled the correlated uncertainties



(a)



(b)

Figure 4: Performance of surrogate models for charge uncertainties for *N,N*-dimethyl-*p*-methoxybenzamide. (a): RMSE for surrogate model with different number of output samples. (b): comparison of the PDFs estimated by the numerical surrogate method (“Numeric”) based on 300 output samples of APBS; dash line (“Experiment”) is the result by the experiment; diamonds are results by using atomic charges from AM1BCC, CHELP, CHELPg, CM2, ESPMK, Gasteiger, PCMESP, Qeq, RESP, MMFF94, Mulliken.

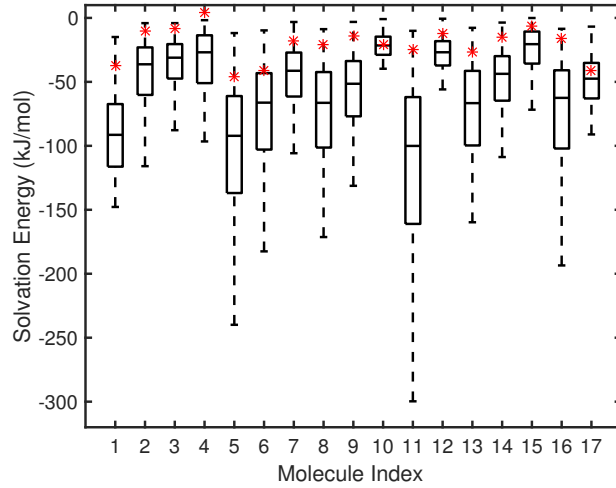


Figure 5: Results of atomic charge uncertainties. Box-whisker plots demonstrating the uncertainties in the numerical results of the solvation energy for 17 compounds. The red stars are the experiment results.

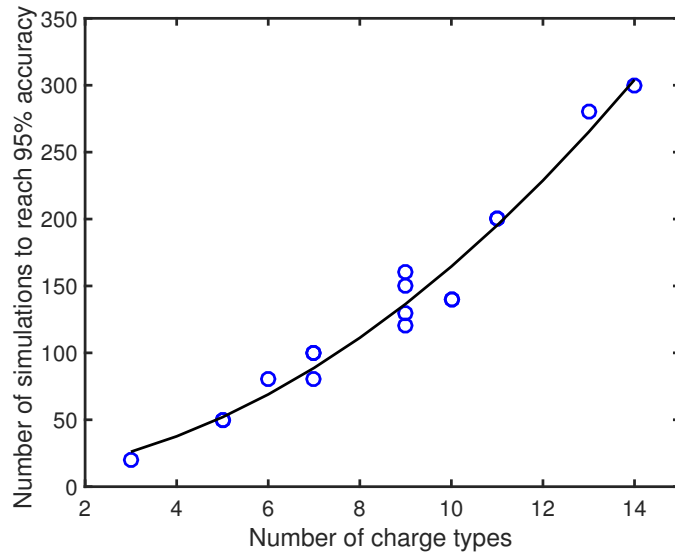


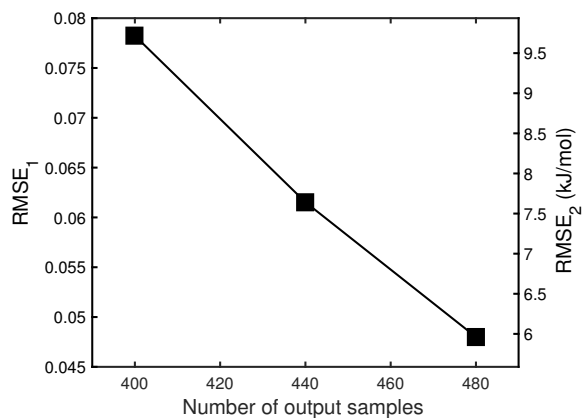
Figure 6: “o” : number of output samples needed to construct a surrogate model with RMSE less than 5% with respect to the number of atom types; “-” is the best-fit curve $1.4x^2 + 1.9x + 7.9$.

for these two types of parameters can be modeled with i.i.d. Gaussian random variables. We use *N,N*-dimethyl-*p*-methoxybenzamide as an example. 480 output samples are needed to reduce the RMSE to less than 5%. Figure 7 (a) presents the RMSE obtained by our method with respect to different numbers of samples E^q . Figure 7 (b) compares the PDF obtained by our method and the reference solution. The numerical results are obtained by constructing the surrogate model from the 480 output samples and then sampling the surrogate model 10,000 times with random samples to estimate the PDF. The reference solution is computed from the 10,000 outputs of E^q . Not surprisingly, the number of output samples needed to construct an accurate surrogate increases as we take into account both uncertainties in the charges and radii. The shape of the solvation energy changes PDF also slightly as the radii variation of the radii across different methods are much smaller than charge variations.

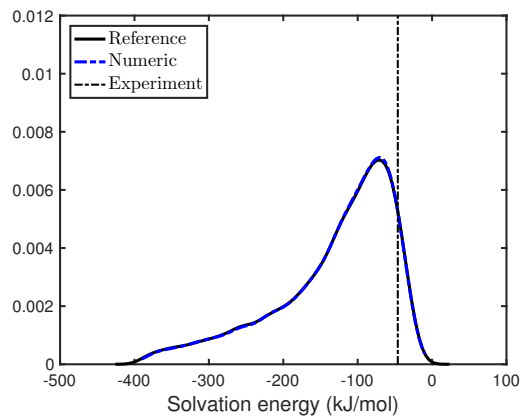
The influences of the uncertainties in the input atomic charges on the solvation energy for each molecule are demonstrated in Figure 8. This figure is similar to Figure 5 since the uncertainties in the atomic charges dominate the results. Figure 9 shows the number of output samples needed to construct a surrogate with less than 5% RMSE for all 17 molecules in the test set. This figure illustrates the approximately quadratic scaling with the respect to the number of atom types in the molecule.

4 Conclusions

We have developed a new method for quantifying the uncertainty associated with parameterization of implicit solvent models. In particular, we used a newly developed extension of compressive sensing method to construct surrogate models of solvation energy based on gPC expansions. These surrogate models allow us to efficiently and accurately estimate the variation in solvation energy due to uncertainty in charge and radius parameters. In this initial work, we used statistical distributions for radius and charge variation based on the observed differences in the parameter sets. However, in future studies, it may be useful to use the uncertainty quantification approach presented here with more physically motivated models that address the underlying uncertainties in determining charge and radius parameters. Our results demonstrate that for the data sets used in the present work, the variation of radii across different approaches are small. On the other hand, the variations of the atomic charges obtained by different methods are much larger, so that the number of output samples needed for accurate UQ analysis requires are much larger, growing quadratically with respect to the number of atom types. This framework can be applied to estimate the statistics (e.g., mean, variance), PDF, confidence interval, Chernoff-like bounds [59], etc. of solvation computing and other chemical computing when the inputs are uncertain. The current study focused on uncertainty in solute charges and radii; however, this framework could also be applied to other solvation model characteristics such as dielectric coefficient, solvent radius, and biomolecular surface definition. Likewise, this approach could also be used for



(a)



(b)

Figure 7: Results of radii and charges uncertainties for *N,N*-dimethyl-*p*-methoxybenzamide. (a): RMSE with different number of output samples M . (b): comparison of the PDFs estimated by the numerical method (“Numeric”) based on 480 output samples of APBS; dashed line (“Experiment”) is the experimental result.

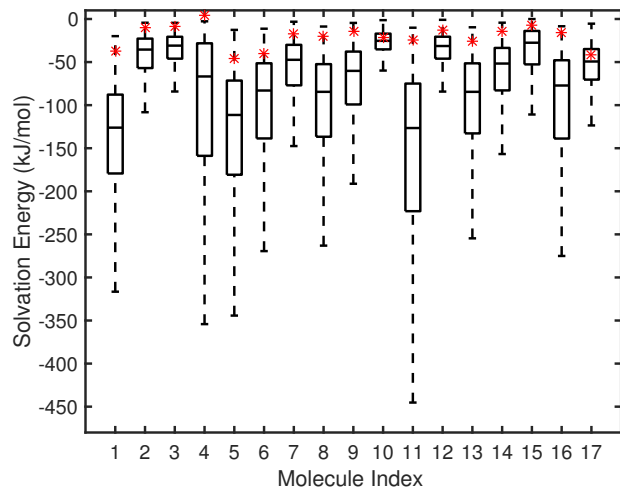


Figure 8: Results of radius and atomic charge uncertainties. Box-whisker plots demonstrating the uncertainties in the numerical results of the solvation energy for 17 compounds. Red stars are the experiment results.

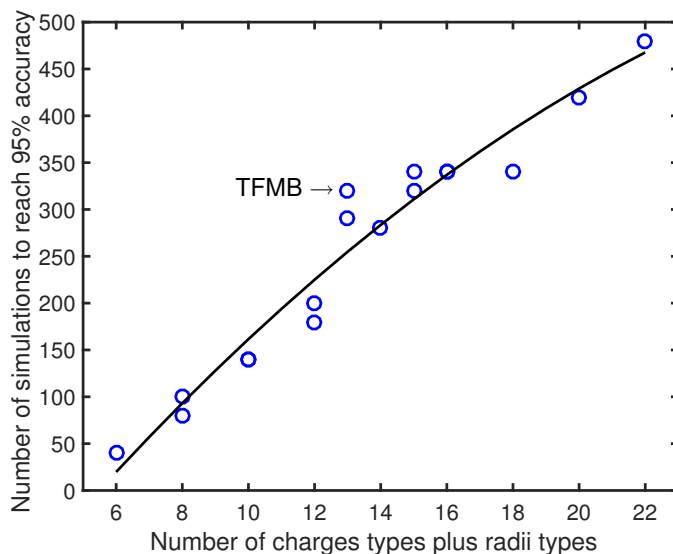


Figure 9: “o” : number of output samples needed to construct a surrogate model with RMSE less than 5% with respect to the number of atom charge types plus radius types; “-” fitting curve $-0.6x^2 + 45x - 188$.

quantities of interest other than solvation energy; e.g., dipole moments, titration states, etc.

In the future, we anticipate that this approach could be used for a much wider range of force field parameterization activities, including both coarse-grained and atomistic representations of biomolecules. Uncertainty quantification methods have begun to be used in force field parameterization of simple alkane systems [60]; this paper demonstrates the ability to extend the methods to higher-dimensional systems with more diversity of atom types. Application of these methods offer the benefit of efficiently characterizing parameter space and understanding the impact of parameter variation on quantities of interest. Additionally, the iterative method we used in the present work is very suitable for this type of problem, as the accuracy of the surrogate models are improved significantly after iterations. Especially, the error of the surrogate models for the atomic charge induced uncertainties are reduced by 40% \sim 50% compared with the standard compressive sensing method. Also, there is significant room for development in the numerical methods. For example, the sparsity-enhancing approaches can be combined with other techniques including improved sampling strategies [61, 62], adaptive basis selection [63, 64], and advanced optimization methods [65, 66]. These approaches improve the accuracy of the compressive sensing method from different aspects. As such, they will help to reduce the number of expensive simulations or quantum mechanics calculations needed for constructing accurate surrogates.

Acknowledgments

This work was supported by the U.S. Department of Energy, Office of Science, Office of Advanced Scientific-Computing Research as part of the Collaboratory on Mathematics for Mesoscopic Modeling of Materials (CM4) and by NIH grant GM069702. Pacific Northwest National Laboratory is operated by Battelle for the DOE under Contract DE-AC05-76RL01830.

References

- [1] Gene Lamm. *The Poisson-Boltzmann Equation*, pages 147–365. John Wiley & Sons, Inc., 2003.
- [2] P. Y. Ren, J. H. Chun, D. G. Thomas, M. J. Schnieders, M. Marucho, J. J. Zhang, and N. A. Baker. Biomolecular electrostatics and solvation: a computational perspective. *Quarterly Reviews of Biophysics*, 45(4):427–491, 2012.
- [3] Pawe Grochowski and Joanna Trylska. Continuum molecular electrostatics, salt effects, and counterion binding: a review of the poisson-boltzmann theory and its modifications. *Biopolymers*, 89(2):93–113, 2008.

- [4] Jay W. Ponder and David A. Case. Force fields for protein simulations. *Advances in Protein Chemistry*, 66:27–85, 2003.
- [5] Luke J. Gosink, Christopher C. Overall, Sarah M. Reehl, Paul D. Whitney, David L. Mobley, and Nathan Andrew Baker. Bayesian model averaging for ensemble-based estimates of solvation free energies. *The Journal of Physical Chemistry B*, page doi:10.1021/acs.jpbc.6b09198, 2016.
- [6] Jessica M. J. Swanson, Stewart A. Adcock, and J. Andrew McCammon. Optimized radii for poissonboltzmann calculations with the amber force field. *Journal of Chemical Theory and Computation*, 1(3):484–493, 2005.
- [7] Chuan Li, Lin Li, Marharyta Petukh, and Emil Alexov. Progress in developing poisson-boltzmann equation solvers. *Molecular based mathematical biology*, 1:42–62, 2013.
- [8] Jessica M. J. Swanson, John Mongan, and J. Andrew McCammon. Limitations of atom-centered dielectric functions in implicit solvent models. *The Journal of Physical Chemistry B*, 109(31):14769–14772, 2005.
- [9] Jessica M. J. Swanson, Jason A. Wagoner, Nathan Andrew Baker, and J. Andrew McCammon. Optimizing the poisson dielectric boundary with explicit solvent forces and energies: Lessons learned with atom-centered dielectric functions. *Journal of Chemical Theory and Computation*, 3(1):170–183, 2007.
- [10] P. W. Bates, G. W. Wei, and Shan Zhao. Minimal molecular surfaces and their applications. *Journal of Computational Chemistry*, 29(3):380–391, 2008.
- [11] Feng Dong and Huan-Xiang Zhou. Electrostatic contribution to the binding stability of protein-protein complexes. *Proteins*, 65:87–102, 2006.
- [12] F. Eckert, M. Diedenhofen, and A. Klamt. Towards a first principles prediction of pk(a): Cosmo-rs and the cluster-continuum approach. *Molecular Physics*, 108(3-4):229–241, 2010.
- [13] Jacopo Tomasi, Benedetta Mennucci, and Roberto Cammi. Quantum mechanical continuum solvation models. *Chemical Reviews*, 105(8):2999–3094, 2005.
- [14] Michael J. Schnieders and Jay W. Ponder. Polarizable atomic multipole solutes in a generalized kirkwood continuum. *Journal of Chemical Theory and Computation*, 3(6):2083–2097, 2007.
- [15] M. J. Schnieders, N. A. Baker, P. Ren, and J. W. Ponder. Polarizable atomic multipole solutes in a poisson-boltzmann continuum. *J Chem Phys*, 126(12):124114, 2007.

- [16] Anthony Nicholls, David L Mobley, J Peter Guthrie, John D Chodera, Christopher I Bayly, Matthew D Cooper, and Vijay S Pande. Predicting small-molecule solvation free energies: an informal blind test for computational chemistry. *Journal of Medicinal Chemistry*, 51(4):769–779, 2008.
- [17] Brent H Besler, Kenneth M Merz, and Peter A Kollman. Atomic charges derived from semiempirical methods. *Journal of Computational Chemistry*, 11(4):431–439, 1990.
- [18] Thomas Haschka, Eric Hénon, Christophe Jaillet, Laurent Martiny, Catherine Etchebest, and Manuel Dauchez. Direct minimization: Alternative to the traditional l2 norm to derive partial atomic charges. *Computational and Theoretical Chemistry*, 1074:50–57, 2015.
- [19] Christopher I Bayly, Piotr Cieplak, Wendy Cornell, and Peter A Kollman. A well-behaved electrostatic potential based method using charge restraints for deriving atomic charges: the resp model. *The Journal of Physical Chemistry*, 97(40):10269–10280, 1993.
- [20] Richard F. W. Bader. A quantum theory of molecular structure and its applications. *Chemical Reviews*, 91(5):893–928, 1991.
- [21] B. Lee and F. M. Richards. The interpretation of protein structures: Estimation of static accessibility. *Journal of Molecular Biology*, 55(3):379–400, 1971.
- [22] M. L. Connolly. Analytical molecular surface calculation. *Journal of Applied Crystallography*, 16(5):548–558, 1983.
- [23] J. Andrew Grant, Barry T. Pickup, and Anthony Nicholls. A smooth permittivity function for poisson-boltzmann solvation methods. *Journal of Computational Chemistry*, 22(6):608–640, 2001.
- [24] W. Im, D. Beglov, and B. Roux. Continuum solvation model: Computation of electrostatic forces from numerical solutions to the poisson-boltzmann equation. *Computer Physics Communications*, 111:59–75, 1998.
- [25] P. W. Bates, Zhan Chen, Yuhui Sun, Guo-Wei Wei, and Shan Zhao. Geometric and potential driving formation and evolution of biomolecular surfaces. *Journal of Mathematical Biology*, 59:193–231, 2009.
- [26] Z. Chen, N. A. Baker, and G. W. Wei. Differential geometry based solvation model I: Eulerian formulation. *J Comput Phys*, 229(22):8231–8258, 2010.
- [27] Li-Tien Cheng, Joachim Dzubiella, J. Andrew McCammon, and Bo Li. Application of the level-set method to the implicit solvation of nonpolar molecules. *The Journal of Chemical Physics*, 127(8):084503–084503, 2007.
- [28] J. Dzubiella, J. M. J. Swanson, and J. A. McCammon. Coupling hydrophobicity, dispersion, and electrostatics in continuum solvent models. 96, 2006.

- [29] J. Dzubiella, J. M. Swanson, and J. A. McCammon. Coupling nonpolar and polar solvation free energies in implicit solvent models. *The Journal of Chemical Physics*, 124(8):84905–84905, 2006.
- [30] Doree Sitkoff, Kim A. Sharp, and Barry Honig. Accurate calculation of hydration free energies using macroscopic solvent models. *The Journal of Physical Chemistry*, 98(7):1978–1988, 1994.
- [31] Roger G. Ghanem and Pol D. Spanos. *Stochastic finite elements: a spectral approach*. Springer-Verlag, New York, 1991.
- [32] Dongbin Xiu and George Em Karniadakis. The Wiener-Askey polynomial chaos for stochastic differential equations. *SIAM J. Sci. Comput.*, 24(2):619–644, 2002.
- [33] Radu Alexandru Todor and Christoph Schwab. Convergence rates for sparse chaos approximations of elliptic problems with stochastic coefficients. *IMA J. Numer. Anal.*, 27(2):232–261, 2007.
- [34] Ivo Babuška, Fabio Nobile, and Raul Tempone. A stochastic collocation method for elliptic partial differential equations with random input data. *SIAM Rev.*, 52(2):317–355, 2010.
- [35] Huan Lei, Xiu Yang, Bin Zheng, Guang Lin, and Nathan A Baker. Constructing surrogate models of complex systems with enhanced sparsity: quantifying the influence of conformational uncertainty in biomolecular solvation. *SIAM Multiscale Model. Simul.*, 13(4):1327–1353, 2015.
- [36] Xiu Yang, Huan Lei, Nathan A Baker, and Guang Lin. Enhancing sparsity of hermite polynomial expansions by iterative rotations. *Journal of Computational Physics*, 307:94–109, 2016.
- [37] Nathan A Baker, David Sept, Simpson Joseph, Michael J Holst, and J Andrew McCammon. Electrostatics of nanosystems: application to microtubules and the ribosome. *Proceedings of the National Academy of Sciences*, 98(18):10037–10041, 2001.
- [38] U Chandra Singh and Peter A Kollman. An approach to computing electrostatic charges for molecules. *Journal of Computational Chemistry*, 5(2):129–145, 1984.
- [39] Araz Jakalian, Bruce L Bush, David B Jack, and Christopher I Bayly. Fast, efficient generation of high-quality atomic charges. AM1-BCC model: I. method. *Journal of Computational Chemistry*, 21(2):132–146, 2000.
- [40] Lisa Emily Chirlian and Michelle Miller Francl. Atomic charges derived from electrostatic potentials: A detailed study. *Journal of Computational Chemistry*, 8(6):894–905, 1987.

- [41] Curt M Breneman and Kenneth B Wiberg. Determining atom-centered monopoles from molecular electrostatic potentials. the need for high sampling density in formamide conformational analysis. *Journal of Computational Chemistry*, 11(3):361–373, 1990.
- [42] Jiabo Li, Tianhai Zhu, Christopher J Cramer, and Donald G Truhlar. New class iv charge model for extracting accurate partial charges from wave functions. *The Journal of Physical Chemistry A*, 102(10):1820–1831, 1998.
- [43] Johann Gasteiger and Mario Marsili. Iterative partial equalization of orbital electronegativity a rapid access to atomic charges. *Tetrahedron*, 36(22):3219–3228, 1980.
- [44] Roberto Cammi and Jacopo Tomasi. Remarks on the use of the apparent surface charges (ASC) methods in solvation problems: Iterative versus matrix-inversion procedures and the renormalization of the apparent charges. *Journal of Computational Chemistry*, 16(12):1449–1458, 1995.
- [45] Anthony K Rappe and William A Goddard III. Charge equilibration for molecular dynamics simulations. *The Journal of Physical Chemistry*, 95(8):3358–3363, 1991.
- [46] Thomas A Halgren. Merck molecular force field. I. basis, form, scope, parameterization, and performance of MMFF94. *Journal of Computational Chemistry*, 17(5-6):490–519, 1996.
- [47] Robert S Mulliken. Electronic population analysis on LCAO-MO molecular wave functions. I. *The Journal of Chemical Physics*, 23(10):1833–1840, 1955.
- [48] Jennifer L. Knight and Charles L. Brooks. Surveying implicit solvent models for estimating small molecule absolute hydration free energies. *Journal of Computational Chemistry*, 32(13):2909–2923, October 2011.
- [49] Guanhua Hou, Xiao Zhu, and Qiang Cui. An implicit solvent model for SCC-DFTB with charge-dependent radii. *J. Chem. Theory Comput.*, 6(8):2303–2314, August 2010.
- [50] Bojana Ginovska, Donald M. Camaioni, Michel Dupuis, Christine A. Schwedtfeger, and Quinn Gil. Charge-Dependent cavity radii for an accurate dielectric continuum model of solvation with emphasis on ions: Aqueous solutes with oxo, hydroxo, amino, methyl, chloro, bromo, and fluoro functionalities. *J. Phys. Chem. A*, 112(42):10604–10613, October 2008.
- [51] Paul Czodrowski, Ingo Dramburg, Christoph A. Sotriffer, and Gerhard Klebe. Development, validation, and application of adapted PEOE charges to estimate pKa values of functional groups in protein-ligand complexes. *Proteins: Structure, Function, and Bioinformatics*, 65(2):424–437, August 2006.

- [52] Qingyi Yang and Kim A. Sharp. Atomic charge parameters for the finite difference Poisson-Boltzmann method using electronegativity neutralization. *J. Chem. Theory Comput.*, 2(4):1152–1167, July 2006.
- [53] William L. Jorgensen, David S. Maxwell, and Julian Tirado-Rives. Development and testing of the opls all-atom force field on conformational energetics and properties of organic liquids. *J. Am. Chem. Soc.*, 118(45):11225–11236, 1996.
- [54] A Bondi. van der waals volumes and radii. *The Journal of Physical Chemistry*, 68(3):441–451, 1964.
- [55] Michael L. Connolly. Computation of molecular volume. *J. Am. Chem. Soc.*, 107(5):1118–1124, March 1985.
- [56] Alexandru M. Micu, Babak Bagheri, Andrew V. Ilin, Ridgway Scott, and Pettitt. Numerical considerations in the computation of the electrostatic free energy of interaction within the PoissonBoltzmann theory. *Journal of Computational Physics*, 136(2):263–271, September 1997.
- [57] Kim A. Sharp and Barry Honig. Calculating total electrostatic energies with the nonlinear Poisson-Boltzmann equation. *J. Phys. Chem.*, 94(19):7684–7692, September 1990.
- [58] Arghya Chakavorty, Lin Li, and Emil Alexov. Electrostatic component of binding energy: Interpreting predictions from poisson-boltzmann equation and modeling protocols. *J. Comput. Chem.*, 37(28):2495–2507, October 2016.
- [59] Muhibur Rasheed, Nathan Clement, Abhishek Bhowmick, and Chandrajit Bajaj. Statistical framework for uncertainty quantification in computational molecular modeling. In *Proceedings of the 7th ACM International Conference on Bioinformatics, Computational Biology, and Health Informatics*, pages 146–155. ACM, 2016.
- [60] Richard A. Messerly, Thomas A. Knotts, and W. Vincent Wilding. Uncertainty quantification and propagation of errors of the lennard-jones 12-6 parameters for n-alkanes. *Journal of Chemical Physics*, 146(19):194110, 2017.
- [61] Holger Rauhut and Rachel Ward. Sparse Legendre expansions via ℓ_1 -minimization. *J. Approx. Theory*, 164(5):517–533, 2012.
- [62] Ji Peng, Jerrad Hampton, and Alireza Doostan. A weighted ℓ_1 -minimization approach for sparse polynomial chaos expansions. *J. Comput. Phys.*, 267(0):92 – 111, 2014.
- [63] Xiu Yang, Minseok Choi, Guang Lin, and George Em Karniadakis. Adaptive ANOVA decomposition of stochastic incompressible and compressible flows. *J. Comput. Phys.*, 231(4):1587–1614, 2012.

- [64] John D Jakeman, Michael S Eldred, and Khachik Sargsyan. Enhancing ℓ_1 -minimization estimates of polynomial chaos expansions using basis selection. *J. Comput. Phys.*, 289:18–34, 2015.
- [65] Emmanuel J. Candès, Michael B. Wakin, and Stephen P. Boyd. Enhancing sparsity by reweighted l_1 minimization. *J. Fourier Anal. Appl.*, 14(5-6):877–905, 2008.
- [66] Xiu Yang and George Em Karniadakis. Reweighted ℓ_1 minimization method for stochastic elliptic differential equations. *J. Comput. Phys.*, 248(1):87–108, 2013.